V Prisma Day, Prato, 17-18 novembre 2023

Identifying parent bodies of meteorites among near-Earth asteroids

A. Carbognani (1), M. Fenucci (2, 3)

(1) INAF - Osservatorio di Astrofisica e Scienza dello Spazio, Via Gobetti 93/3, 40129 Bologna, Italy
(2) ESA ESRIN / PDO / NEO Coordination Centre, Largo Galileo Galilei, 1, 00044 Frascati (RM), Italy
(3) Elecnor Deimos, Via Giuseppe Verdi, 6, 28060 San Pietro Mosezzo (NO), Italy

INAF
ISTITUTO NAZIONALE
DI ASTROFISICA

Prima Rete Italiana Sorveglianza Sistematica Meteore & Atmosfera
PRISMA

Meteorite’s origin

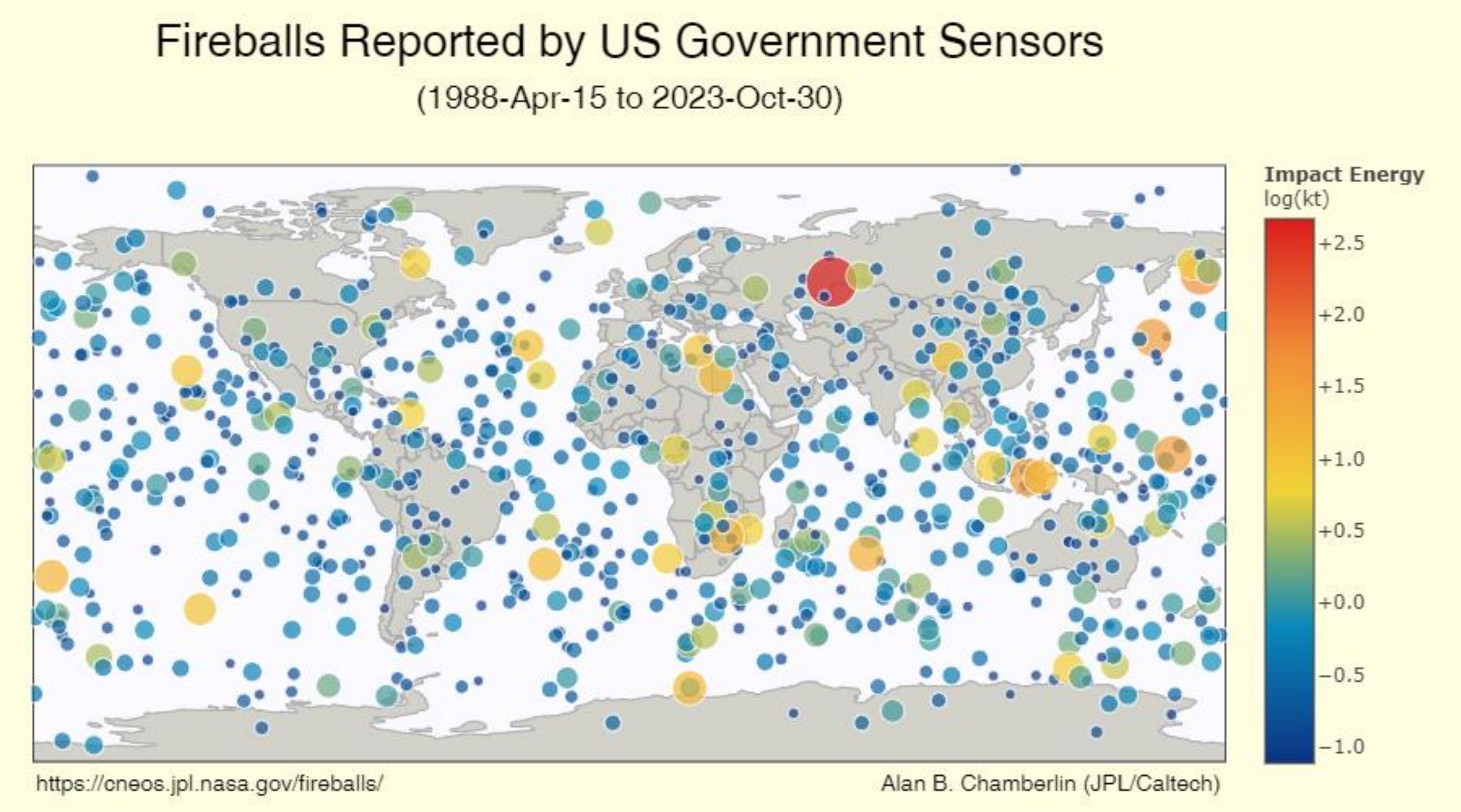

Small bodies continuously bombard the Earth’s atmosphere.

According to NASA's CNEOS data center, there is an event detectable by military satellites on average **every two weeks**, with a **mean diameter of about 1-2 m**.

About 9.8% of the events belong to **Jupiter Family Comets**, while 85.5% have a Tisserand parameter with respect to Jupiter, **typical of <u>asteroid orbits</u>**.

There are **no known meteorites of cometary origin**.

Meteorite’s progenitor bodies are unknown

- Meteorites originate from the asteroid population, but it is difficult to identify which are the progenitors. The asteroid **Vesta** and meteorites of the **HED** (Howardite-Eucrite-Diogenite) type are notable exceptions.
- The progenitor bodies of the **ordinary chondrites** (OC) which make up about 80% of the falls, are **S-type asteroids**, but they are not yet identified with certainty. OCs must have originated from **at least three progenitor bodies** to explain the presence of chondrites of type H (42.5% of the OCs), L (46.2%) and LL (11.3%) according to the decreasing content of iron and metals.

Meteorites from Main-Belt

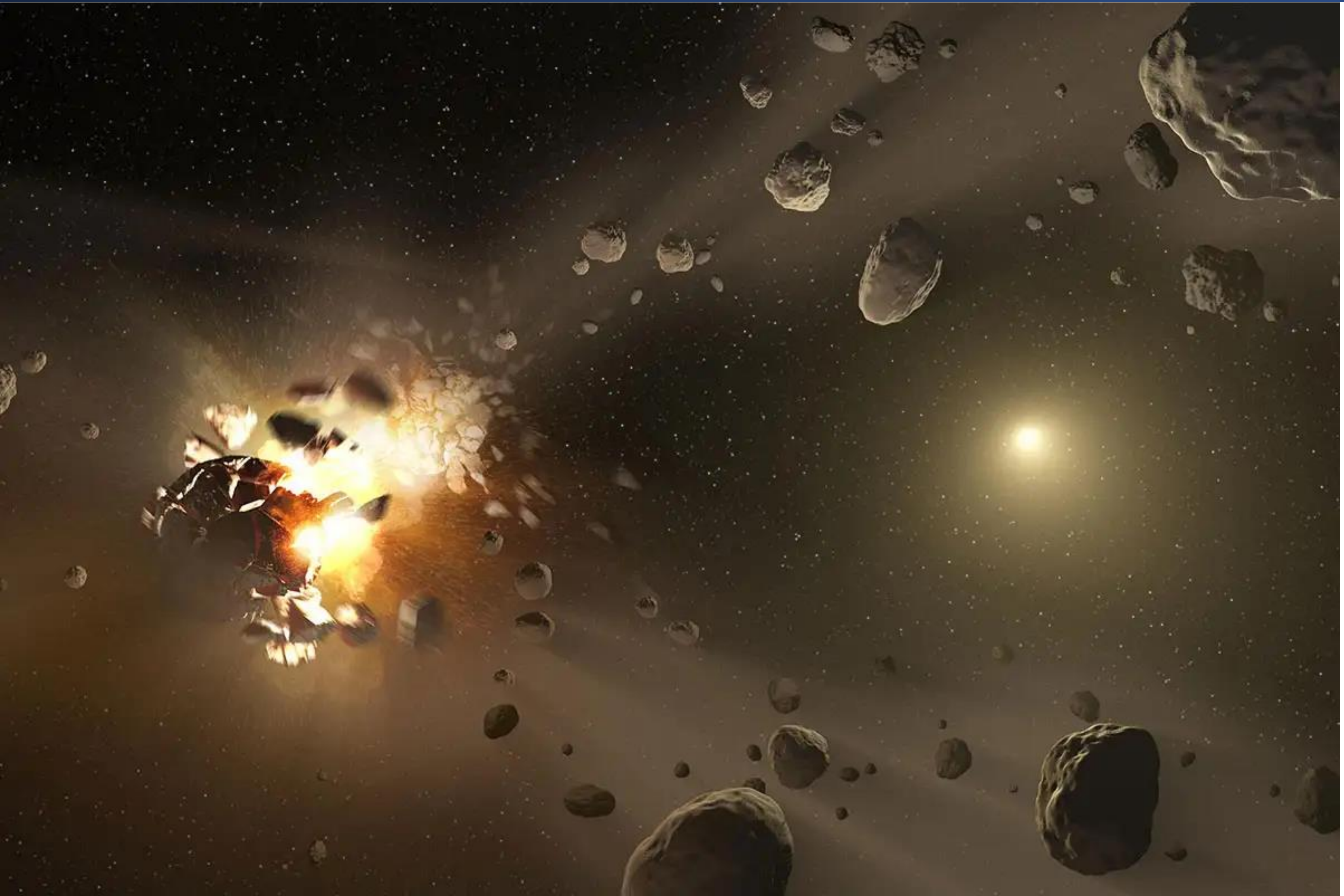

According to the **current paradigm**, the **progenitor meteoroids** of meteorites were formed millions of years ago following collisions between main-belt asteroids that created **asteroid families**.

Subsequently, due to the **mean-motion orbital resonances with Jupiter** and the **Yarkovsky effect**, they were placed on near-Earth-type orbits, which led them to fall on Earth.

(1) The prominent **Flora family** in the inner part of the main belt is a good candidate to be the origin of rare **LL-type ordinary chondrites**.

(2) S-type asteroid **(6) Hebe**, located adjacent to 3:1 mean-motion resonance with Jupiter, is the probable source of **H-type OC**.

Meteorite orbits are rare

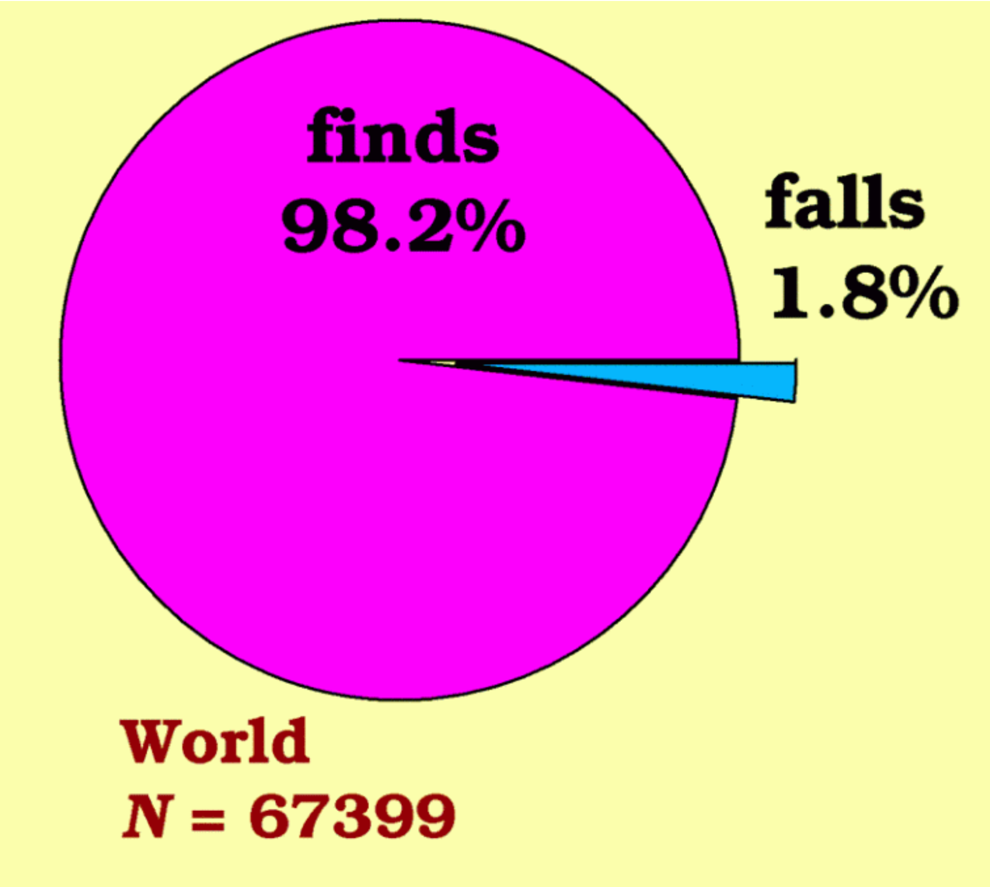

There are only about 45 known orbits of meteorite-associated meteoroids, a very small fraction of the meteorites collected on the Earth, about 1/1500.

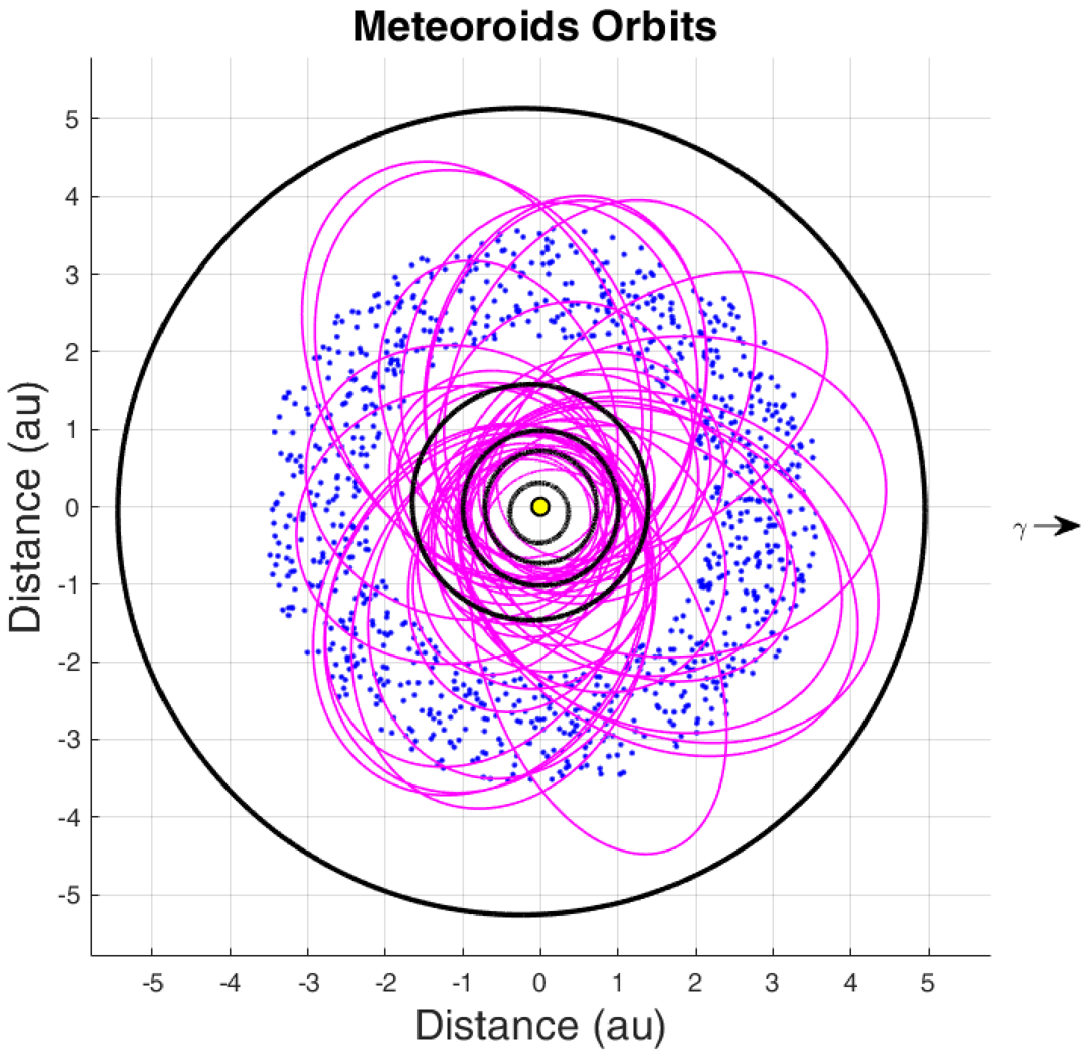

Table 1. List of meteorites with a heliocentric orbit from fireball triangulation sorted by date of fall in Julian days (JD): a = semimajor axis; e = eccentricity; i = orbit inclination; Ω = longitude of ascending node; ω = argument of perihelion; M = mean anomaly of the fall. Orbital elements for equinox J2000.0. Meteorite type: OC = ordinary chondrite; C = carbonaceous chondrite; EC = enstatite chondrite; AE = achondrite eucrite; AH = achondrite howardite; U = ureilite. In this table, meteorite type are from the Meteoritical Bulletin Database (https://www.lpi.usra.edu/meteor/). For an extensive set of references regarding this list of meteorites, you can consult the Meteorite Orbits.info website (https://www.meteoriteorbits.info/). These data bases were last consulted on 2023 May 10.

N	Name	Type	a (au)	e	i (°)	Ω (°)	ω (°)	M (°)	JD fall
01	Pribram	OC H5	2.40 ± 0.002	0.6711 ± 0.0003	10.482 ± 0.0004	17.79147 ± 0.00001	241.75 ± 0.013	349.539	2436666.333
02	Lost City	OC H5	1.66 ± 0.05	0.417 ± 0.005	12.0 ± 0.5	283.0 ± 0.5	161.0 ± 0.5	7.182	2440591.333
03	Innisfree	OC L5	1.87 ± 0.005	0.4732 ± 0.0005	12.27 ± 0.05	316.80 ± 0.05	177.97 ± 0.05	0.640	2443181.292
04	Benesov	OC LL3.5	2.48 ± 0.002	0.6274 ± 0.0004	23.981 ± 0.007	47.0009 ± 0.0001	218.370 ± 0.008	352.417	2448384.458
05	Peekskill	OC H6	1.49 ± 0.03	0.41 ± 0.01	4.9 ± 0.2	17.030 ± 0.001	308.0 ± 1.0	21.540	2448905.292
06	Tagish Lake	C2-ung	2.1 ± 0.2	0.57 ± 0.05	1.4 ± 0.9	297.900 ± 0.003	222.0 ± 2.0	349.895	2451561.833
07	Moravka	OC H5	1.85 ± 0.07	0.47 ± 0.02	32.2 ± 0.5	46.2580 ± 0.00005	203.5 ± 0.6	352.385	2451671.042
08	Neuschwanstein	EC EL6	2.40 ± 0.02	0.670 ± 0.002	11.41 ± 0.03	16.82664 ± 0.00001	241.20 ± 0.06	349.420	2452371.347
09	Park Forest	OC L5	2.53 ± 0.19	0.680 ± 0.023	3.2 ± 0.3	6.1156 ± 0.0007	237.5 ± 1.6	350.715	2452725.493
10	Villalbeto de la Peña	OC L6	2.3 ± 0.2	0.63 ± 0.04	0.0 ± 0.2	283.6712 ± 0.00005	132.3 ± 1.5	9.229	2453009.199
11	Bunburra Rockhole	AE	0.85 ± 0.0004	0.2427 ± 0.0005	8.95 ± 0.03	297.595 ± 0.0005	210.04 ± 0.06	133.571	2454302.301
12	Almahata Sitta	U	1.308201 ± 0	0.31206 ± 0	2.54220 ± 0	194.101138 ± 0	234.44897 ± 0	330.834	2454746.615
13	Buzzard Coulee	OC H4	1.25 ± 0.02	0.23 ± 0.02	25.0 ± 0.8	238.93739 ± 0.00008	211.3 ± 1.4	340.573	2454791.518
14	Maribo	CM2	2.43 ± 0.2	0.805 ± 0.011	0.25 ± 0.16	297.46 ± 0.15	279.4 ± 0.6	348.713	2454849.299
15	Jesenice	OC L6	1.75 ± 0.07	0.431 ± 0.022	9.6 ± 0.5	019.196 ± 0.0005	190.5 ± 0.5	356.220	2454930.583
16	Grimsby	OC H5	2.04 ± 0.05	0.518 ± 0.011	28.07 ± 0.28	182.9561 ± 0.00005	159.865 ± 0.43	5.548	2455100.544
17	Košice	OC H5	2.71 ± 0.24	0.647 ± 0.032	2.0 ± 0.8	340.072 ± 0.004	204.2 ± 1.2	355.951	2455256.434
18	Mason Gully	OC H5	2.470 ± 0.004	0.6023 ± 0.009	0.832 ± 0.013	203.2112 ± 0.00005	218.95 ± 0.03	351.810	2455299.941
19	Križevci	OC H6	1.544 ± 0.01	0.521 ± 0.004	0.64 ± 0.03	315.55 ± 0.01	254.4 ± 0.1	335.381	2455597.472
20	Sutter's Mill	C	2.59 ± 0.35	0.824 ± 0.02	2.38 ± 1.16	32.77 ± 0.06	77.8 ± 3.2	10.452	2456040.118
21	Novato	OC L6	2.088 ± 0.077	0.526 ± 0.017	5.508 ± 0.040	24.99 ± 0.0035	347.352 ± 0.134	3.360	2456218.613
22	Chelyabinsk	OC LL5	1.72 ± 0.02	0.571 ± 0.006	4.98 ± 0.12	326.459 ± 0.001	107.67 ± 0.17	20.000	2456338.640
23	Annama	OC H5	1.99 ± 0.12	0.69 ± 0.02	14.65 ± 0.46	28.611 ± 0.001	264.77 ± 0.55	344.111	2456766.426
24	Žd'ár nad Sázavou	OC L3	2.093 ± 0.006	0.6792 ± 0.001	2.796 ± 0.009	257.262 ± 0.010	257.721 ± 0.014	345.583	2457001.178
25	Porangaba	OC L4	2.45 ± 1.10	0.64 ± 0.11	8.6 ± 3.2	288.921 ± 0.001	142.8 ± 6.7	6.638	2457032.232
26	Sariçiçek	AH	1.454 ± 0.083	0.304 ± 0.039	22.6 ± 1.6	159.849 ± 0.004	182.8 ± 1.6	358.576	2457268.342
27	Creston	OC L6	1.300 ± 0.019	0.410 ± 0.013	4.228 ± 0.070	30.458 ± 0.006	7.20 ± 0.13	323.239	2457319.741
28	Murrili	OC H5	2.521 ± 0.075	0.609 ± 0.012	3.32 ± 0.060	64.742 ± 0.0033	354.557 ± 0.039	1.050	2457353.947
29	Ejby	OC H5/6	2.81 ± 0.09	0.65 ± 0.011	0.96 ± 0.10	317.211 ± 0.0001	197.75 ± 0.10	357.102	2457425.380
30	Stubenberg	OC LL6	1.525 ± 0.010	0.395 ± 0.004	2.07 ± 0.03	346.520 ± 0.0001	221.02 ± 0.03	342.834	2457454.400
31	Dishchii'bikoh	OC LL7	1.129 ± 0.008	0.205 ± 0.004	21.24 ± 0.27	72.1206 ± 0.0002	108.7 ± 1.5	50.231	2457541.955
32	Dingle Dell	OC LL6	2.254 ± 0.034	0.5905 ± 0.0063	4.051 ± 0.012	218.252 ± 0.00032	215.773 ± 0.049	352.191	2457693.002
33	Hamburg	OC H4	2.73 ± 0.05	0.661 ± 0.006	0.604 ± 0.11	296.421 ± 0.03	211.65 ± 0.3	354.949	2458135.547
34	Motopi Pan	AH	1.3764 ± 0.0001	0.43186 ± 0.00006	4.2974 ± 0.0004	71.869605 ± 0.000012	256.04869 ± 0.00055	327.170	2458272.197
35	Ozerki	OC L6	0.84 ± 0.02	0.199 ± 0.03	18.443 ± 3.047	89.656 ± ?	335.286 ± 5.147	215.712	2458290.553
36	Viñales	OC L6	1.217 ± 0.005	0.391 ± 0.005	11.47 ± 0.05	132.28 ± 0.005	276.97 ± 0.05	306.489	2458516.262
37	Arpu Kuilpu	OC H5	2.75 ± 0.03	0.671 ± 0.003	2.03 ± 0.01	250.36 ± 0.01	43.25 ± 0.02	353.166	2458635.912
38	Flensburg	C1	2.82 ± 0.03	0.701 ± 0.003	6.82 ± 0.06	349.207 ± 0.001	307.25 ± 0.16	7.480	2458739.035
39	Cavezzo	OC L5-an	1.82 ± 0.22	0.46 ± 0.063	4.0 ± 1.6	280.52311 ± 0.00001	179.2 ± 4.8	0.261	2458850.268
40	Novo Mesto	OC L5	1.451 ± 0.004	0.6086 ± 0.0006	8.755 ± 0.063	338.993041 ± 0.00001	82.649 ± 0.184	28.826	2458907.896
41	Madura Cave	OC L5	0.889 ± 0.003	0.327 ± 0.009	0.12 ± 0.08	88.703764 ± 0.00001	312.02 ± 0.51	260.842	2459020.336
42	Traspena	OC L5	1.125 ± 0.016	0.386 ± 0.013	4.55 ± 0.19	297.8270 ± 0.0003	273.93 ± 0.98	309.939	2459232.514
43	Winchcombe	CM2	2.5855 ± 0.0077	0.6183 ± 0.0011	0.460 ± 0.014	160.1955 ± 0.0014	351.798 ± 0.018	1.524	2459274.410
44	Antonin	OC L5	1.1269 ± 0.0007	0.2285 ± 0.0006	24.22 ± 0.05	112.5807 ± 0.0001	257.16 ± 0.09	307.227	2459410.625

Why not meteorites from NEAs?

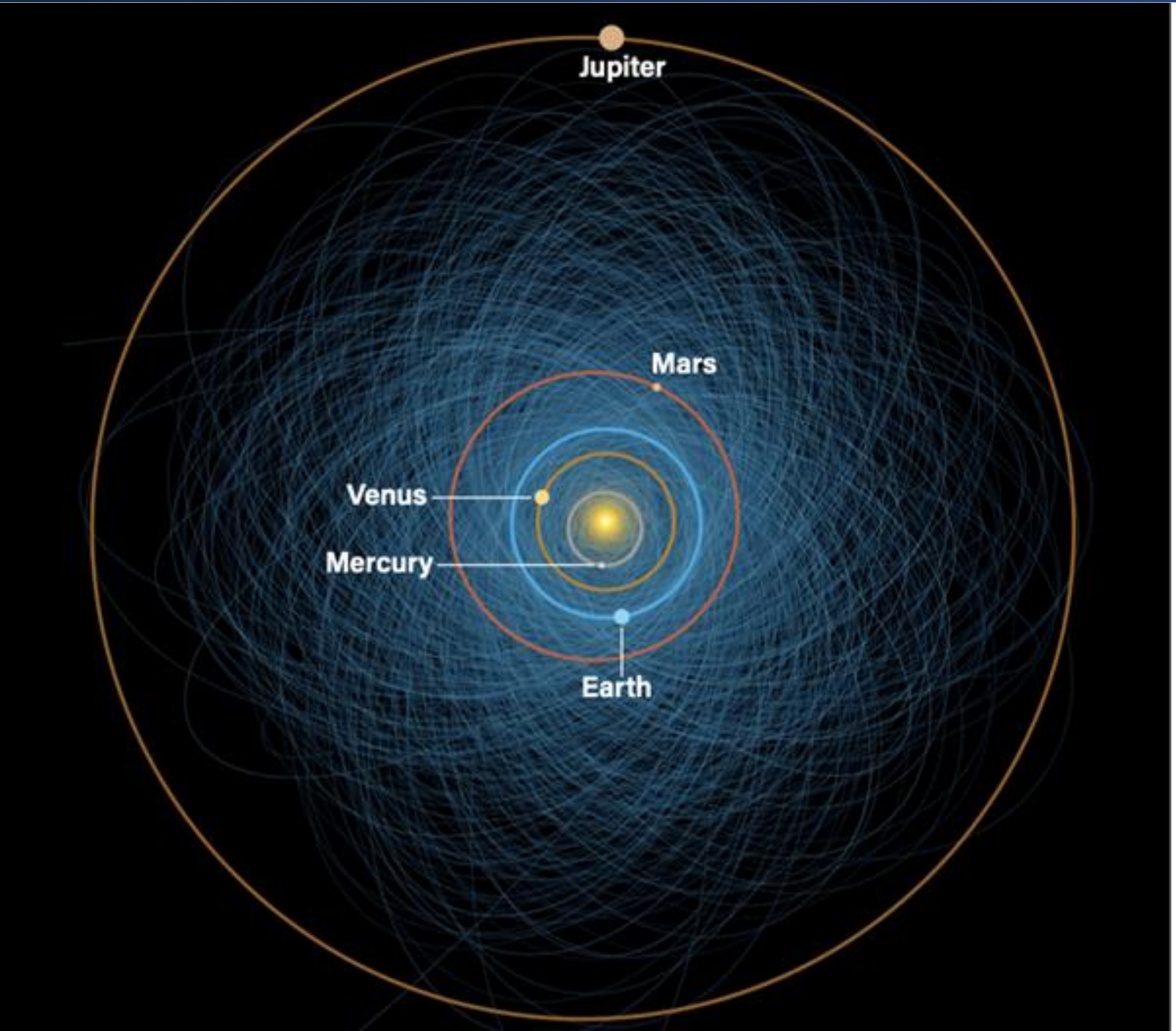

It cannot be excluded that a part of the meteorites originates directly from the dynamic **population of the near-Earth asteroids** (NEAs). Possible formation mechanisms:

(1) Collisions with smaller NEAs.

(2) Thermal fragmentation (Phaethon).

(3) Partial rotational disaggregation of rubble piles due to the YORP effect (binary, pairs).

(4) Tidal disruption of rubble piles during flyby with planets.

(5) Sublimation of small reserves of volatile materials.

Cavezzo meteoroid: orbit with minimum D_N value

A **<u>dissimilarity criterion</u>** is used to search for a connection between the observed orbits of the meteors and the progenitor body.

D_N depends on four geocentric quantities directly related to the observations:
(1) **U**, the geocentric speed of the body.
(2) The angles **θ** and **ϕ** are directly related to the radiant.
(3) **λ**, the heliocentric longitude of the Earth at the encounter with the meteor.

- Cavezzo's orbit is compatible with the orbit of one object only among currently known NEOs: **2013 VC_{10}**

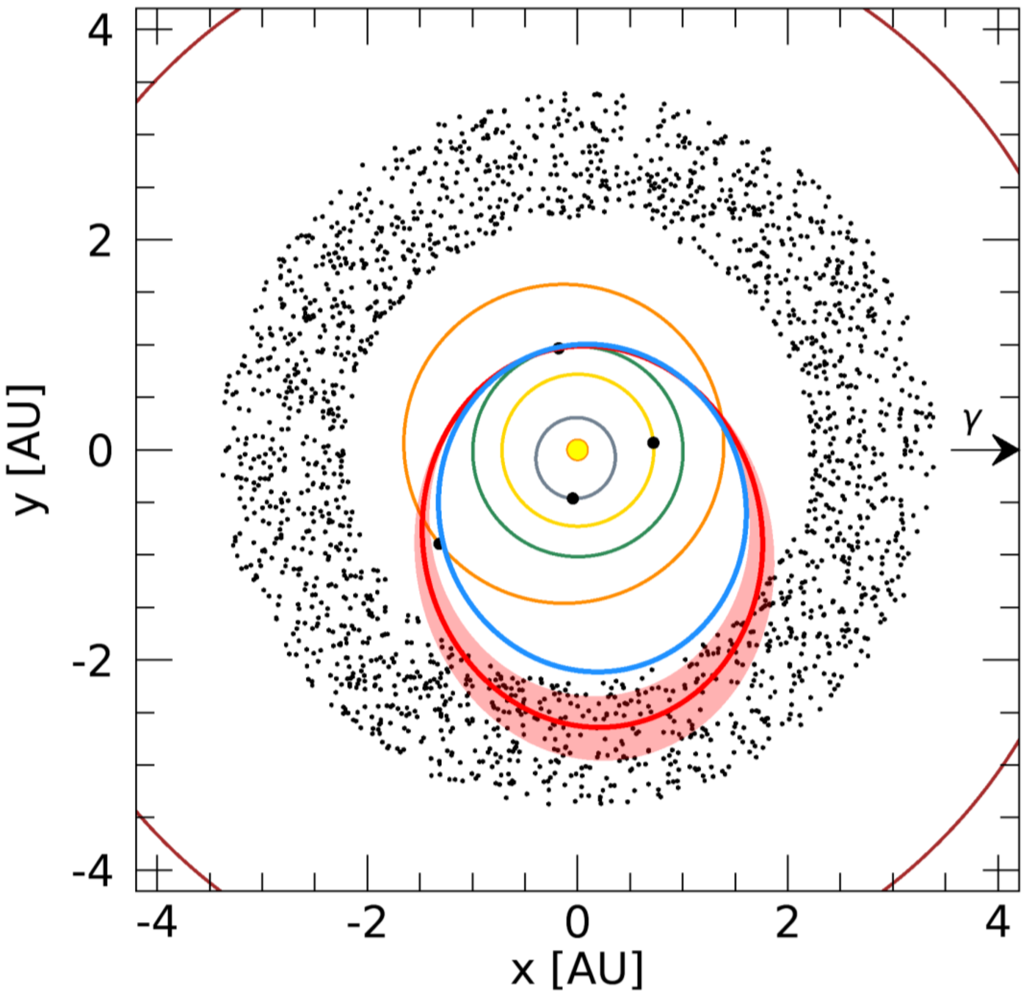

The true geocentric all-sky radiants distribution for NEAs and meteorites

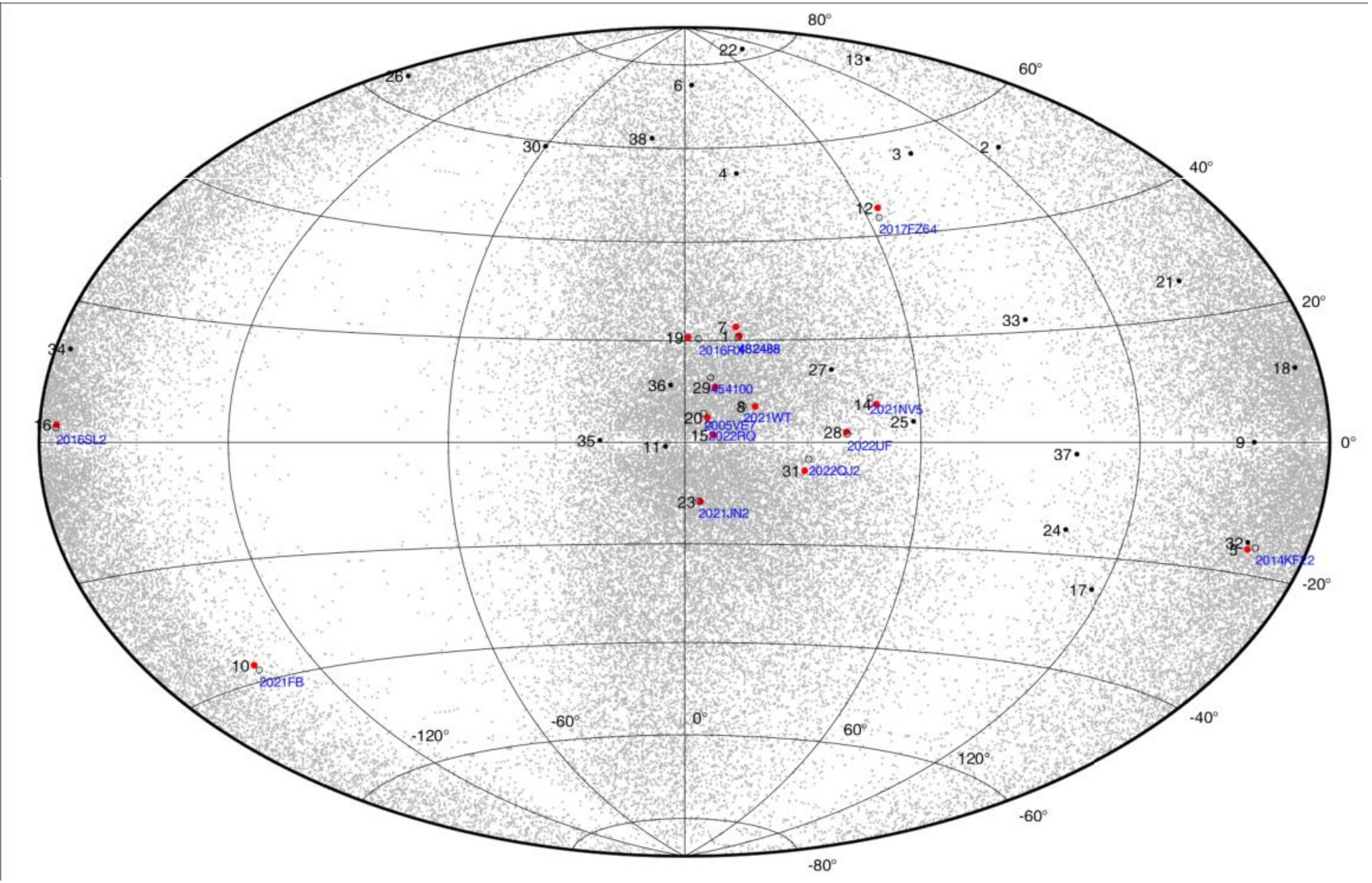

List of meteorites with an associated NEA with **D_N ≤ 0.06**.

Meteorite Name	NEA	Diam. (m)	T_J	C	DN
Pribram	482488	300–600	3.109	0.3	0.047
Peekskill	2014 KF22	15–30	4.444	5.9	0.041
Neuschwanstein	482488	300–600	3.109	0.3	0.056
Park Forest	2021 WT	30–60	3.178	7.6	0.053
Bunburra Rockhole	2021 FB	20–40	6.942	6.4	0.042
Jesenice	2017 FZ64	40–100	3.736	7.8	0.055
Košice	2021 NV5	10–20	3.234	6.8	0.049
	2019 ST2	50–120	3.288	9.0	0.059
Križevci	2022 RQ	20–50	4.472	7.9	0.044
	2013 BR15	30–60	4.280	9.0	0.056
Sutter's Mill	2016 SL2	30–60	3.327	8.7	0.050
Annama	2016 RX	20–40	2.943	7.1	0.048
Žd'ár nad Sázavou	2005 VE7	500–1200	3.156	0.5	0.048
Creston	2021 JN2	40–100	5.328	7.0	0.055
Hamburg	2022 UF	10–20	3.110	6.8	0.057
	2021 PZ1	20–40	3.279	7.6	0.043
Motopi Pan	454100	500–600	4.824	0	0.044
	2017 MC3	40–100	4.333	3.5	0.046
	2009 FZ4	20–50	5.535	2.0	0.055
Arpu Kuilpu	2022 QJ2	20–50	3.067	8.2	0.057

In search of a common origin

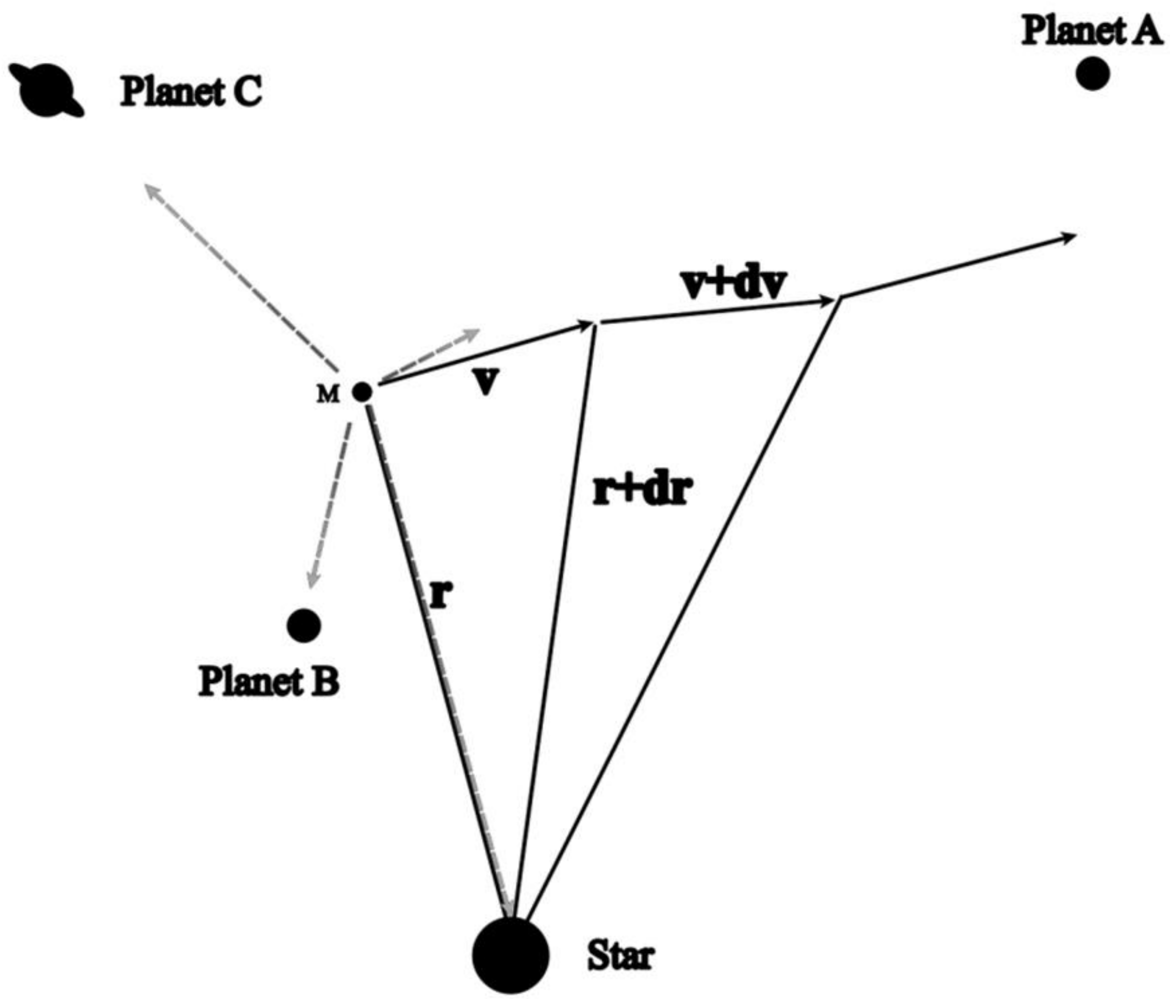

For NEA orbits, the most important **gravitational perturbations** of the time-averaged **disturbing function** can be **secular**, i.e. independent of the average longitude on the orbit, **resonant** like those that give rise to Kirkwood gaps, or **short-term** if they cannot be classified into the first two types.

Secular perturbations act on a time scale of thousands of years, and can be seen in the **values of the longitude of the perihelion and the ascending node, which can increase or decrease linearly over time** and in those of the eccentricity and inclination, which instead oscillate almost sinusoidally. The semi-major axis remains constant under secular perturbations.

To understand whether it is possible to determine a candidate age for the separation between the meteorite and the proposed parent body, we searched for convergence events involving a small relative velocity and a small distance between the two objects.

$$d = \sqrt{\left(\frac{\mathrm{MOID}}{\mu(\mathrm{MOID})}\right)^2 + \left(\frac{\Delta V}{\mu(\Delta V)}\right)^2},$$

Pribram (1957) – Neuschwanstein (2002)

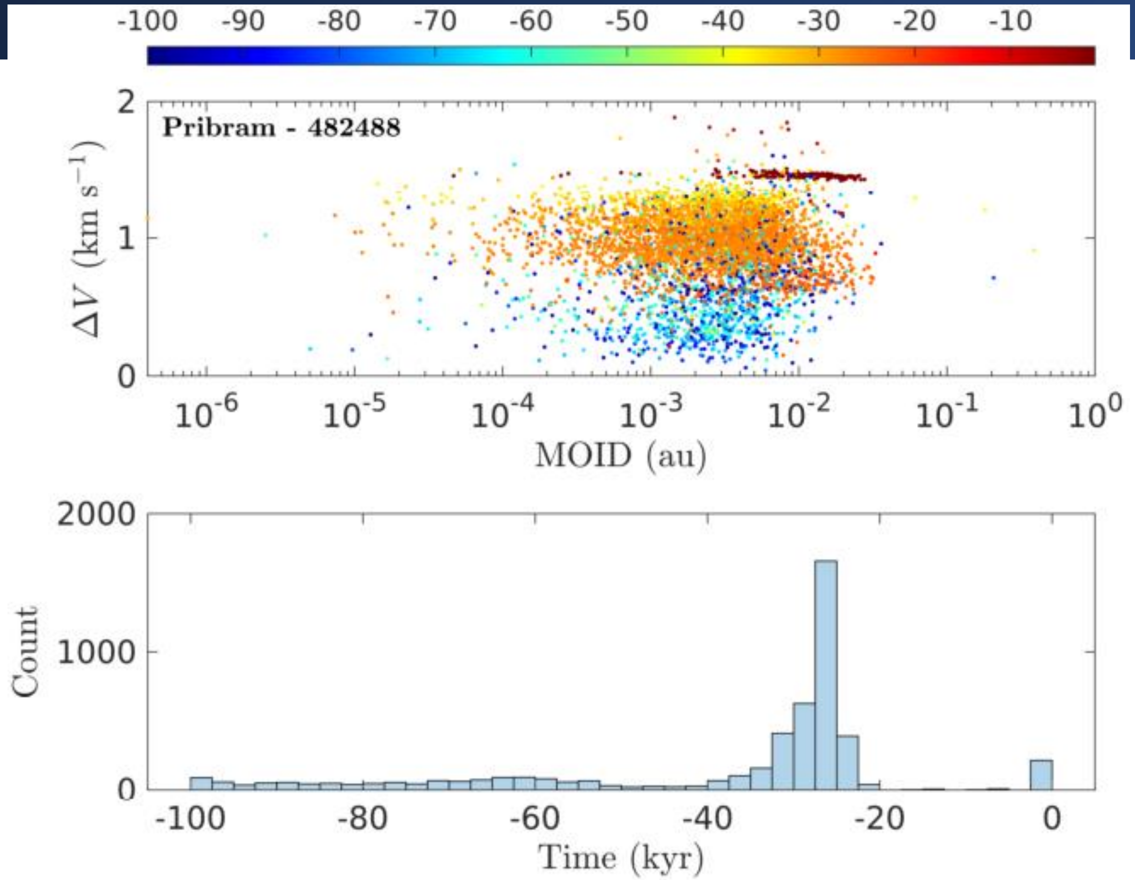

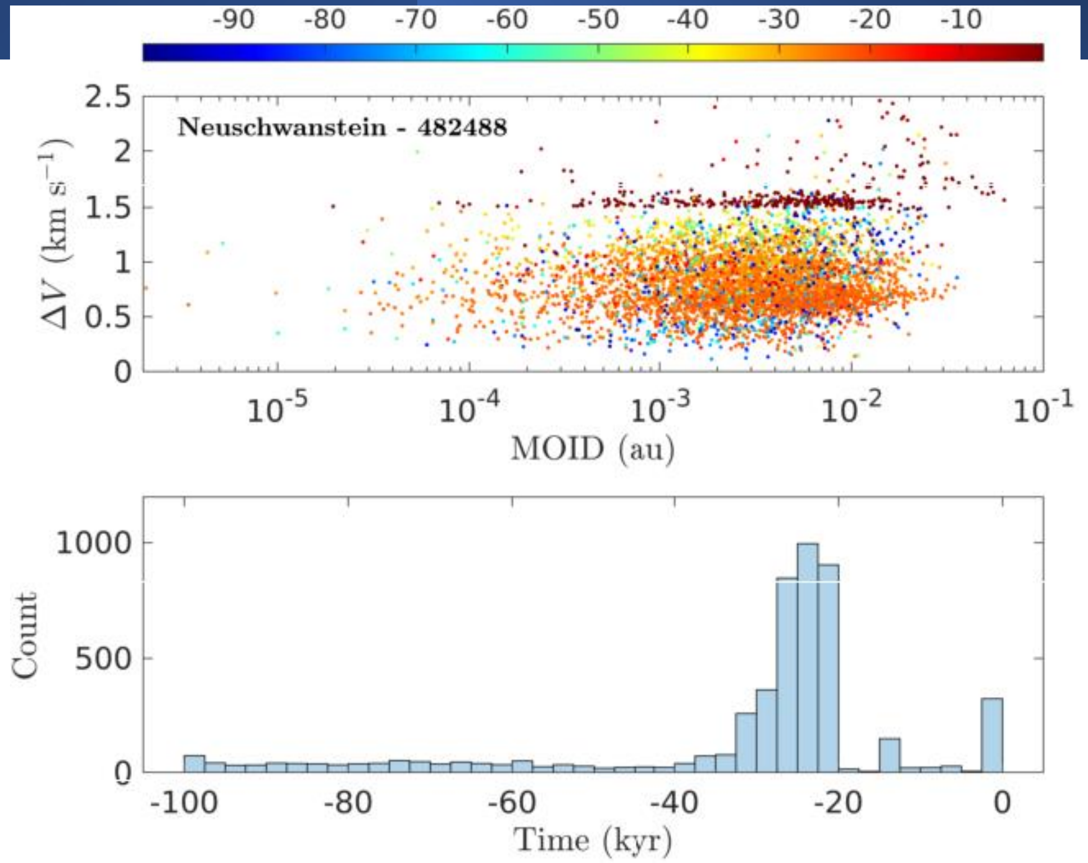

In the case of Pribram and Neuschwanstein, the **age of separation** from the asteroid 482488 appears similar, -**20/-30 kyr**, so they were probably born in the **same impact event**. The **cosmic-ray exposure times** of the two meteorites are different (**12 Myr Pribram**, **48 Myr Neuschwanstein**), but this does not prevent them from having a common origin. Most likely 482488, considering the diameter, is a **rubble pile asteroid** as Bennu, made up of **blocks with very different and complex exposure histories**.

Motopi Pan (2018 LA)

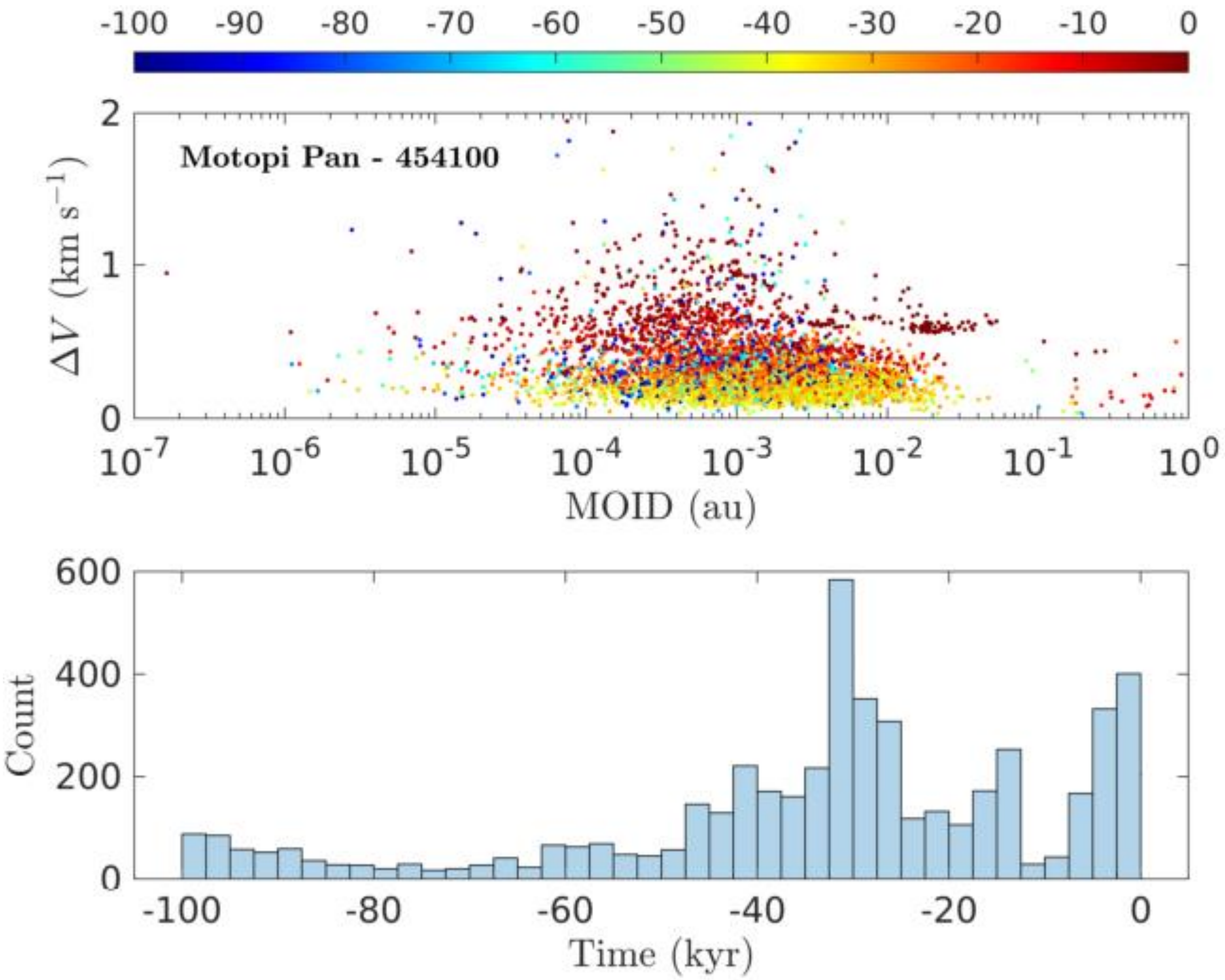

Two concentrations appear between 0 and -5 kyr and at around -30 kyr of evolution, however, their statistics are poor.

Overall, only a few per cent of minima are achieved after roughly 50 kyr of dynamical evolution, and therefore we could only conclude that the separation event most likely happened in the last 50 kyr.

Also for Motopi Pan the cosmic-ray exposure time is high and estimated to be 19.2 ± 2.4 Myr.

Results: separation age for pairs meteorites-NEA

Table 4. List of the candidate pairs meteorites-NEA with the possible separation age, minimum MOID and minimum ΔV. Note that for all the meteorites with high orbital inclinations Pribram, Neuschwanstein, Bunburra, Jesenice and Annama it was possible to establish a separation event. I=Inconclusive results, S=spurious association.

Meteorite Name	NEA	Age (kyr)	MOID (au)	ΔV (km s^{-1})
Pribram	482488	$-30/-25$	$10^{-4}-10^{-3}$	1
Peekskill	2014 KF22	-2.5	$10^{-4}-10^{-2}$	0.8
Neuschwan.	482488	$-25/-20$	$10^{-4}-10^{-3}$	1
Park Forest	2021 WT	S	-	-
Bunburra Rockhole	2021 FB	S	-	-
Jesenice	2017 FZ64	-10 or -17	$10^{-5}-10^{-2}$	1
Košice	2021 NV5	I	-	-
	2019 ST2	I	-	-
Križevci	2022 RQ	-7.5	$10^{-6}-10^{-3}$	6
	2013 BR15	S	-	-
Sutter's Mill	2016 SL2	-2.5	$10^{-4}-10^{-1}$	0.5
Annama	2016 RX	-2.5 or -35	$10^{-3}-10^{-1}$	4 or 3
Žd'ad S.	2005 VE7	I	-	-
Creston	2021 JN2	$-7.5/5$	$10^{-5}-10^{-2}$	3.5
Hamburg	2022 UF	$-10/0$	$10^{-4}-10^{-1}$	1
	2021 PZ1	S	-	-
Motopi Pan	454100	$-2.5/-30$	$10^{-5}-10^{-2}$	< 0.5
	2017 MC3	-5	$10^{-5}-10^{-2}$	5
	2009 FZ4	-10	$10^{-6}-10^{-2}$	1
Arpu Kuilpu	2022 QJ2	S	-	-

The orbital evolution of **20 pairs** was studied starting from the time of the fall and going back in time.
To account for the greater uncertainty of meteorite orbital elements with respect to NEAs, a population of 5000 clones was used for each meteorite. Results:

(1) For **12 of these potential pairs**, concentrations of distance minima were found in the phase space formed by the MOID of the orbits and by the relative speed at MOID.

(2) The **minimum MOID between the orbits is around 10^{-4} au** (15000 km), while the **relative velocity is about 1 km/s**.

(3) **Time scales** of the order of **tens of thousands of years (~10000 yr)** for the NEA-meteorite separation time.

(4) The relative speed of about 1 km/s suggests that **collision events** separated the meteorite from the parent NEA.

Collision frequency between little NEAs is compatible with NEA-meteorite separation time

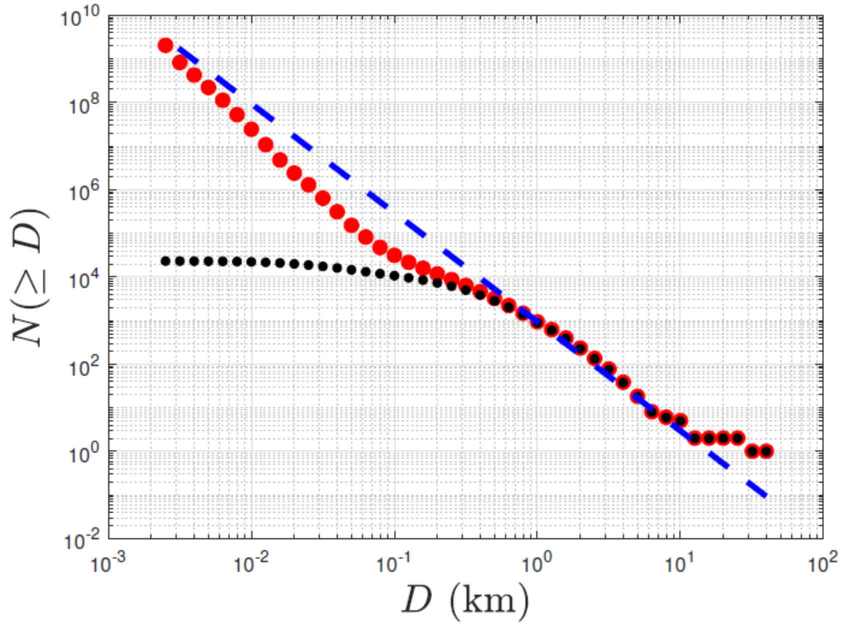

Figure 12. A log-log plot of the NEAs cumulative diameter distribution according to Harris & Chodas (2021) model (red dots) and the observed ones (black dots). The dashed blue line is the simple power law $N(\geq D) = 940 \times D^{-2.5}$. This exponential law is what one would expect in the case of a population of bodies that has undergone a collisional evolution in which the destructive process depends only by the collision speed and the size ratio between the colliding bodies (de Pater & Lissauer 2010). The constant 940 normalizes it to the Harris & Chodas (2021) model for asteroids 1 km in diameter or larger.

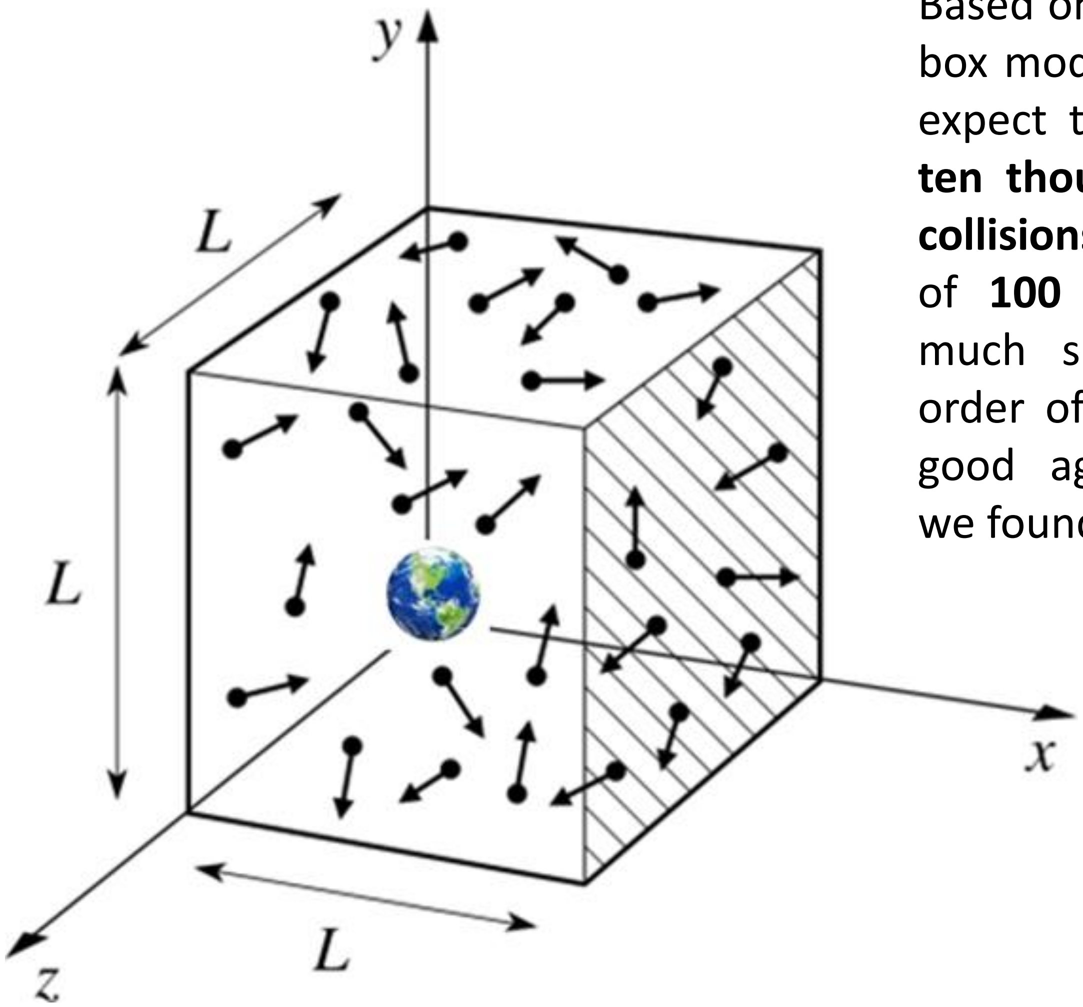

Based on a simple NEA-in-the-box model, it is reasonable to expect times of the order of **ten thousand years** between **collisions of NEAs** of the order of **100 m in diameter** and much smaller NEAs of the order of **2 m in diameter**, in good agreement with what we found.

Conclusions

(1) It seems reasonable to assume that the population of micro-NEAs collide with small NEAs, generating a part of the meteorites found on Earth.

(2) Our **starting sample** consisted of **38 meteorites**, but only 10 of them appear associated with a known NEA, which means that about **10/38 ≈ 25%** of the meteorites probably **originate directly in the NEA population**, mainly from **little collision events** in the inner Solar System, **rather than from asteroid collisions in the main belt**.

(3) In summary, the collisions that occur in the main belt can also continue to **occur between the NEAs**, generating a **minority part of the meteorites that we find on Earth**.

THANK YOU FOR YOUR ATTENTION!

Carbognani A., Fenucci M., **Identifying parent bodies of meteorites among near-Earth asteroids**
Monthly Notices of the Royal Astronomical Society, Volume 525, Issue 2, October 2023, Pages 1705–1725,
https://doi.org/10.1093/mnras/stad2382